

# Brain Tumor Segmentation Based on Structuring Element Map Modification and Marker-controlled Watershed Transform

Xiaopeng Wang, Shengyang Wan, Tao Lei

School of Electronic and Information Engineering, Lanzhou Jiaotong University, Lanzhou, 730070, China

Email: wangxp1969@sina.com

**Abstract**—Brain medical images are generally prone to noise and also fraught with intensity heterogeneity within the tumor. Fuzzy and boundary discontinuity caused by the tumor also adversely affects the accuracy of the tumor segmentation. A method based on morphological structuring element map modification and marker-controlled watershed segmentation is proposed. Firstly, a structuring element map is constructed according to the sum of the weighted variance of the specific regions within morphological gradient image, and each value of the structuring element map represents the size of structuring element (SE). Secondly, the original image is modified by morphological opening-closing, where the size of SE are determined by the structuring element map in the corresponding pixel, such an adaptive image modification can eliminate the noise and small regular details while preserve the larger object contours without less location offsets. Finally, marker-controlled watershed transform is used to complete the tumor segmentation. Experiments show that the method ensures brain tumors are more accurately segmented.

**Index Terms**—image segmentation, brain tumor, structuring element map, marker-controlled watershed transform

## I. INTRODUCTION

Incidence of brain tumors has been on the rise in recent years. According to statistics, brain tumor accounts for about 5% of the human tumor cases and also forms about 60% of children tumor cases. About 20-30% of other malignant tumors also eventually land into intracranial categories. Because of its invasive growth, expansion in intracranial domains, once it occupies a certain space, regardless of its nature being benign or malignant, are bound to make the intracranial pressure suppress brain tissues, leading to injury to the central nervous system, thus endangering patient's life. Brain tumor's early detection greatly depends on the accurate diagnosis and subsequently its effective treatment. The accuracy of the result is thus a very important step to improving the disease treatment. MR and CT technologies are widely applied in the diagnosis and analysis of brain tumors. These technologies render brain tumor location

information in the form of size and type, and can be used for brain tumor resection surgery and radiation therapy as important information.

Many efforts have been made to segment brain tissue and tumor from MR and CT Images [1-4]. Watershed transform [5, 6] can be used to produce single pixel width and closed contour, etc. and has been widely applied to medical image segmentation [7, 8]. However, the watershed easily leads to over-segmentation [9]. Usually, there are three kinds of schemes to eliminate over-segmentation. The first one is image pre-filtering [10], which uses filters to reduce local minima area before the watershed segmentation. The second one employs the marker-controlled method [11, 19] to limit the segment regions beforehand; the last is the post-processing after watershed, such as region merging [12]. Nowadays, several methods have been proposed for the brain tumor segmentation [1-3, 13-15], Wang [2] introduced a parametric fluid vector flow active contour model to address the issues of limited capture range and use it to implement the brain tumor segmentation; Corso [3, 13] employed multilevel segmentation and integrated Bayesian model classification to separate the brain tumor. Kowar [14] presented a method for the detection of brain tumor using histogram thresholding; Christ [15] applied K-Means clustering integrated with marker-controlled watershed algorithm to segment MR brain images; In fact, the brain tissue structure is more complex, and the boundary of tumor region and normal tissue is not obvious. The CT or MR image itself may contain noise and low-contrast regions, such a case likely cause discontinuities and fuzzy boundaries, and maybe lead to resultant inaccurate segmentation of contours. We thus present a novel method by applying morphological structuring element map to modify the original image, then use the marker-controlled watershed transform to segment the modified image. During the segmentation process, the selection of the appropriate size of SE is the forte of morphological modification. For each pixel of the original image, we apply opening-closing with different SE to modify each pixel, where the size of the SE is determined by the structuring element map.

Manuscript received March 16, 2014; revised May 15, 2014; accepted July 1, 2014.

Corresponding author: Xiaopeng Wang, wangxp1969@sina.com

II. MORPHOLOGICAL MODIFICATION

When applying the marker-controlled watershed transformation to segment the image of brain tumors, it can accurately mark the tumor area and produce closed contours, yet usually the tumor can be present in normal brain tissue. In a variety of medical imaging of tumor shape, the gray value of the interior is not uniform; sometimes the tumor and surrounding tissues are very close resulting in a less accurate segmentation. If the image does not undergo pre-filtering or smoothing, a direct use of marker-controlled watershed transform may result in inaccurate target contour positioning.

Morphological opening and closing can eliminate the bright and dark regions less than the SEs. But the problem is that when apply opening and closing with invariant smaller SE to modify the tumor image, some bright and dark regular details can not be eliminated completely. In reverse, lager SE may lead to the tumor contour occur location offset. To this end, we present a method based on morphological opening and closing to modify image, where the SE's size is variant for the different pixel. The modification mainly based on morphology theory [6,17] is such that, every gray image can be seen as a three-dimensional topographical map, and then using different viscous fluids that are in a flooded landscape. When the viscosity is at a low temperature, the fluid can reach more irregular detailed regions, conversely, when the viscosity is at a high temperature, the fluid can only reach the wider region. Closing operation can eliminate dark regions smaller than SE, this would be equivalent to use different size of the SEs to effect modification of the image by a morphological closing. On the other hand, opening can eliminate bright regions smaller than the SE. The combination of the two operations will release the bright and dark small details and noise within the image, and largely reduce the factors that result in over-segmentation. The gradient can reflect the degree of the image's gray change, but sometimes the pixel's gradient does not accurately reflect the topography image information, therefore, we employ the sum of pixel's gradient weighted gradient variance to determine the size of SE that corresponding to viscosity.

A. Structuring Element Map

For ease and exactly of calculation, the normalization processing is carried out. In the following sections, we will use the normalized images everywhere. The morphological gradient is given by

$$g = (f \oplus s) - (f \ominus s) \tag{1}$$

where  $s$  is a circular SE with 1 as the radius,  $g$  is the gradient image, and  $f$  is the original image,  $\oplus$  and  $\ominus$  respectively denote morphological dilation and erosion.

For the aim to modify each pixel using variant SE, we construct a circular structuring element map  $M(x, y)$ , its size is equal to original image and each pixel value represents the size of the SE which will be used to modify original image in corresponding pixel. Each SE's size in  $M(x, y)$  is determined by the morphological gradient

image. If the gradient image is seen as a topography map, gradient value would represent the altitude of each point, in general the target contour points corresponds to higher elevations. It is well known that the variance is a measure of how far a set of numbers is spread out. For example, a pixel  $A(x, y)$  is shown in Fig. 1. The sum of the square difference of each pixels gradient with  $A$  can reflect the difference between the regions of the  $A$ 's  $3 \times 3$  neighborhood. The sum of the variance is defined as following.

$(x-1, y-1)$	$(x-1, y)$	$(x-1, y+1)$
$(x, y-1)$	$(x, y)$	$(x, y+1)$
$(x+1, y-1)$	$(x+1, y)$	$(x+1, y+1)$

Figure1.  $3 \times 3$  neighborhood.

$$V(x, y) = (g(x-1, y-1) - g(x, y))^2 + (g(x-1, y) - g(x, y))^2 + (g(x-1, y+1) - g(x, y))^2 + (g(x, y-1) - g(x, y))^2 + (g(x, y+1) - g(x, y))^2 + (g(x+1, y-1) - g(x, y))^2 + (g(x+1, y) - g(x, y))^2 + (g(x+1, y+1) - g(x, y))^2 \tag{2}$$

where  $V(x, y)$  denotes the sum of variance,  $g(x, y)$  is the corresponding gradient value. The distance between pixel  $A$  to each neighborhood is different, therefore its impact on the target point varies. If the distance is shorter, the impact is greater and vice versa. Therefore the weighted variance is thus defined as

$$V(x, y) = w_1(g(x-1, y-1) - g(x, y))^2 + w_2(g(x-1, y) - g(x, y))^2 + w_3(g(x-1, y+1) - g(x, y))^2 + w_4(g(x, y-1) - g(x, y))^2 + w_5(g(x, y+1) - g(x, y))^2 + w_6(g(x+1, y-1) - g(x, y))^2 + w_7(g(x+1, y) - g(x, y))^2 + w_8(g(x+1, y+1) - g(x, y))^2 \tag{3}$$

where  $w_i$  denotes the weighting coefficient and is defined as following.

$$w_i = \frac{1}{r} \tag{4}$$

where  $r$  is the distance between the current point  $(x, y)$  to the neighborhood point  $(x', y')$ , and the distance is

$$r = \sqrt{(x-x')^2 + (y-y')^2} \tag{5}$$

Equation (6) reflects the relationship between the weighted variance and structuring elements map.

$$M(x, y) = \lfloor -\log(\alpha \times V(x, y)) \rfloor, \quad (0 \leq M(x, y) \leq R_{\max}) \tag{6}$$

where  $\lfloor \bullet \rfloor$  indicates rounding,  $\alpha$  is a factor to adjust the value of  $M(x, y)$ ,  $R_{\max}$  is the maximal size of SE.

B. Image Modification

Morphological opening-closing operation employs different SE to modify each pixel of the image, and this is different from the traditional opening-closing by fixed SE. Such an adaptive opening-closing operation will eliminate the small bright and dark details and maintain

the accuracy of the larger object contours. Our morphological modification is defined as

$$f_d(x, y) = g(x, y) \circ M(x, y) \bullet M(x, y) \quad (7)$$

where  $f_d(x, y)$  is the modification image,  $\circ$  and  $\bullet$  are respectively denote morphological opening and closing operation.

### III. CONTROLLED WATERSHED

Small regular details are largely eliminated after the image modification. In order to segment the brain tumors and limit the allowable divided regions, marker-controlled watershed is employed to segment the modification image by the following steps.

*Step 1, Tumor Marker Extraction:* The purpose of this step is to locate the inner tumor regions. Since markers are picked from original modified image and the brain tumor regions usually have higher gray values than other brain tissue [20], the tumor regions can be extracted by thresholding( $T$ ) processing, where pixels value larger than  $T$  are labeled as tumor markers  $M$ .

*Step 2, Background Marker Extraction:* In order to determine the inside and outside catchments basins, background markers are also needed. This can be achieved by calculating the watershed transform of the Euclidian distance of the inner tumor regions. The Euclidian distance [19] is defined as following.

$$D_{(i,j)} = \min_{(x,y) \in M} D[(i, j), (x, y)] \quad (8)$$

$$D[(i, j), (x, y)] = \sqrt{(i-x)^2 + (j-y)^2} \quad (9)$$

where  $D_{(i,j)}$  denotes the minimal distance between tumor marker pixel  $(x, y)$  and other pixel  $(i, j)$ ,  $D[(i, j), (x, y)]$  is the Euclidian distance between pixel  $(x, y)$  and  $(i, j)$ .

*Step3, Watershed segmentation:* After the foreground and background markers respectively corresponding to inside and outside of tumor have both marked out, minima imposition is applied to modify the gradient image so that the regional minimum occur at the markers location. Finally, watershed transform is performed on the modified gradient image to implement the tumor segmentation.

### IV. IMPLEMENTATION

Fig.2 shows the proposed segmentation process, firstly, the morphological gradient image is calculated from the original image, and then the sum of variance is computed according to the pixel value of the gradient image. After constructing a structuring elements map with the size equal to the original image, its value of each pixel can be determined by the sum of variance. Modify each pixel of the original image by the different SE that size corresponding to the structuring element map at same location. Then mark the modified gradient image by the foreground and background markers. Finally watershed transform is used to implement the tumor segmentation.

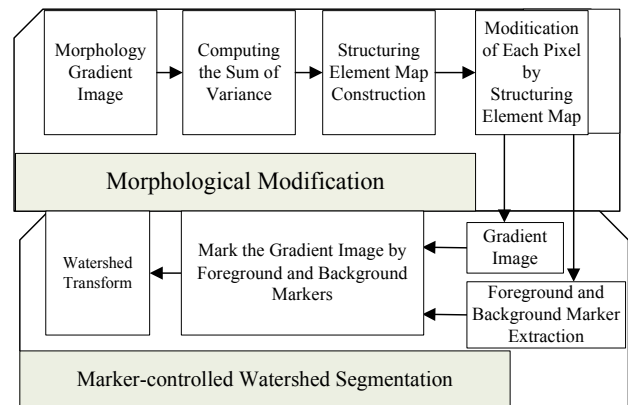


Figure2. The flow chart of the proposed segmentation

### V. EXPERIMENTS AND DISCUSSION

In order to verify the validity and performance of the proposed method, we choose a synthetic image and several clinical brain tumor CT images, and implement the simulation on MATLAB7 platform. The synthetic image as shown of Fig. 3(a), it contains four regions labeled as A1, A2, A3 and A4.

Fig. 3(b) is the result of watershed transform on Fig. 3(a), it produces a serious over-segmentation. Fig. 3(c) shows the segmentation of watershed transform followed by the maximal similarity based region merging [16], it can be seen that over-segmentation is largely released, but object contours occur offset. Fig.3 (d) gives the marker-controlled watershed segmentation, where  $T = 0.15$ . It is obvious that the bottom right corner of A1 is missing, and the other object shape contour is not accurate. Fig. 3(e) shows the result of the proposed modification, where  $R_{max} = 10$  and  $\alpha = 6$ . The marker of gradient image of the modified image by the foreground and background with  $T = 0.05$  is given as Fig. 3(f); the marker-controlled watershed was performed on Fig. 3(f) producing the final segmentation. Compared with manual segmentation as Fig. 3(h), the proposed method result as shown in Fig. 3 (g) has accurately segmented the four desired object contours.

For the purpose to test the performance of the proposed method under noisy condition, we add Gaussian noise (0.1%) and salt-and-pepper noise (5%) to the Fig. 3(a). We can see from Fig. 4(b) when watershed transform is directly applied on such a noisy image, a serious over-segmentation appears. The maximal similarity based region merging is sensitive to noise and produce under-segmentation (Fig. 4(c)). Sole marker-controlled watershed shown in Fig. 4(d) led to inaccurate shape contours, especially, in low-contrast regions. Our method shown from Fig. 4(e) to (f) indicates that it is more robust to noise. TABLE I shows the time-costing of the different segmentation methods, where watershed transform is fast, watershed with region merging is more time-costing, and our method is slower than watershed transform but faster than region merging.

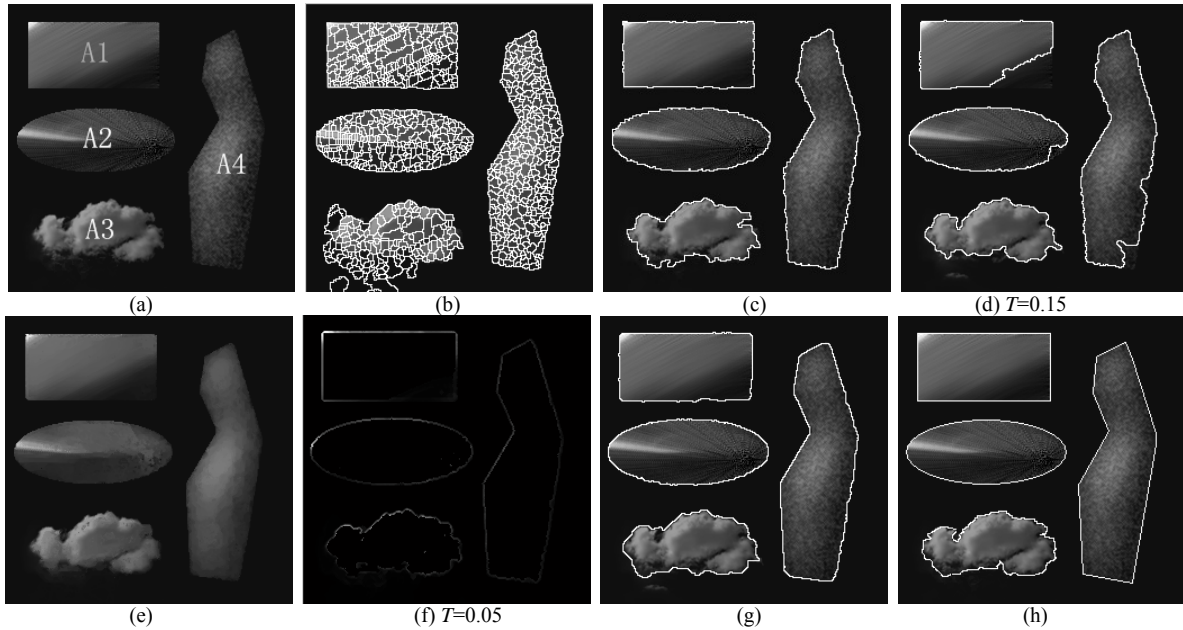


Figure3. The flow chart of the proposed segmentation: The method for segmenting different shapes. (a) The original images; (b) Watershed segmentation; (c) The result of region merging of Fig. 3(b); (d) The result of maker-controlled watershed transform; (e) The result of modification; (f) Maker the gradient image; (g) The proposed segmentation result. (h) Manual segmentation.

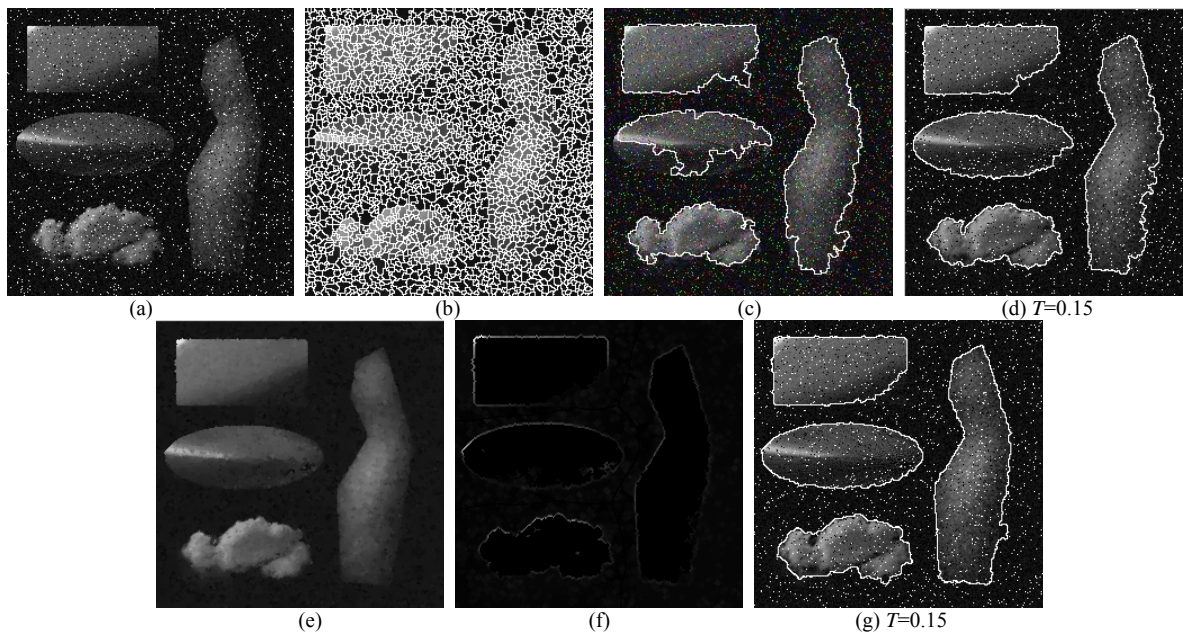


Figure4. The method for segmenting different shapes with noise. (a) Noisy image of Fig. 3(a); (b) Watershed transform for noisy image; (c) The result of region merging of Fig. 4(b); (d) The result of maker-controlled watershed transform; (e) The result of modification, (f) Maker the gradient image; (g) The proposed segmentation result.

TABLE I  
THE TIME-COSTING OF DIFFERENT SEGMENTATION

Image	Segmentation Time(s)		
	Watershed Transform	Region Merging	Proposed method
Figure3 (a)	0.6523	1.5482	9.8764

In order to quantitatively analyze the segmentation accuracy of the different methods, we introduce the *TM* (Tanimoto Metric) [2] to evaluate the results of the segmentation, it is defined as following.

$$TM = \frac{\|R_x \cap R_g\|}{\|R_x \cup R_g\|}, \quad (0 \leq TM \leq 1) \tag{10}$$

where  $R_x$  denotes the amount of the segmented regions,  $R_g$  is the amount of region by hand-sketched,  $\|\bullet\|$  denotes the total number of pixels within the collection. Typically, if *TM* is more close to 1, it indicates that the result of region is more close to the real contour. TABLE II shows the *TM* of the different segmentation methods for four objects in Figure.3 and Figure 4.

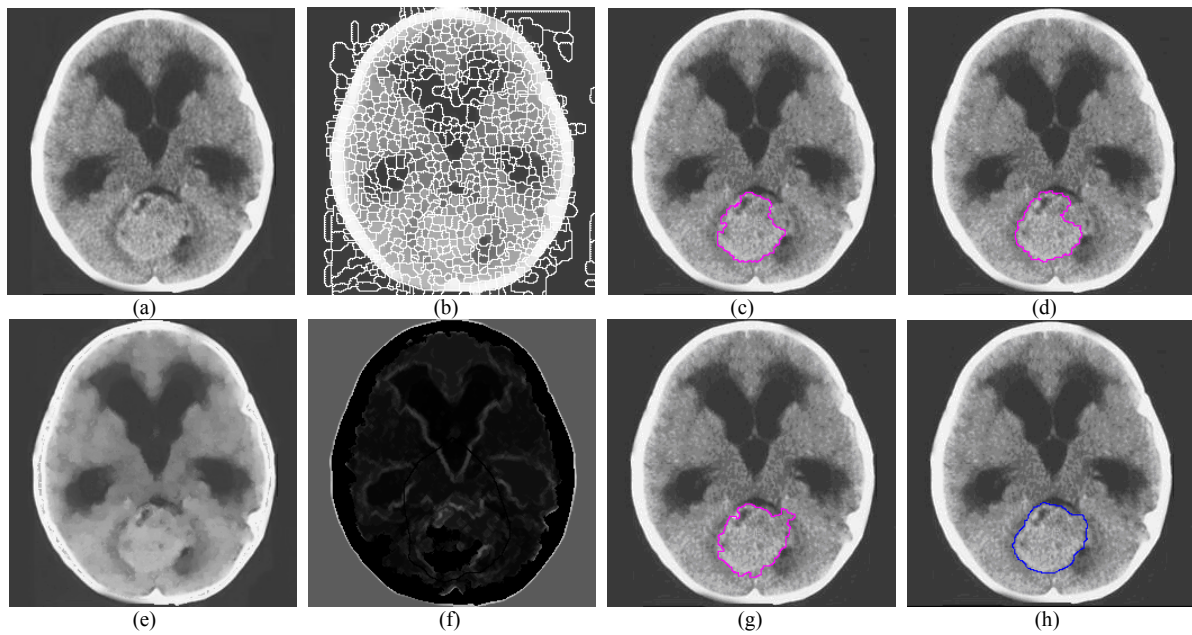


Figure5. Segmentation of CT-1 by different methods. (a)The original image; (b) Watershed transform; (c) Region merging of Fig.5(b); (d) Marker-controlled watershed transform; (e) Modification; (f) Marker the gradient image; (g) The proposed segmentation; (h) Manual segmentation.

TABLE.II  
TM FOR DIFFERENT SEGMENTATION METHODS

Image	TM		
	Region merging	Marker-controlled watershed	Proposed method
Original	A1	0.9376	0.8104
	A2	0.9785	0.9109
	A3	0.9201	0.8778
	A4	0.9683	0.9290
Noisy	A1	0.7343	0.8361
	A2	0.6289	0.9126
	A3	0.8176	0.8726
	A4	0.6688	0.8856

TABLE.III  
TM VALUE FOR DIFFERENT IMAGES

Tumor image	TM
a1	0.9164
a2	0.9273
a3	0.9418
a4	0.8978
a5	0.9102

It indicates that the accuracy of the proposed method is superior to the others, especially in noisy condition. To validate the performance of our method to segment the brain tumor, we firstly choose a clinical CT image named CT-1 as Fig.5(a). Fig.5(b) is the direct segmentation by watershed transform; Fig.5(c) shows the result after the maximal similarity based region merging, where most part of the tumor region is separated from the brain tissue, but the contour location occur bias. The marker - controlled watershed transform is almost the same as shown in Figure 5(d). Our method from Fig.5(e) to (g) indicates that it is closer to the manual segmentation (Fig.5(h)) than the others, where  $R_{max} = 10$ ,  $T = 0.5$  and  $\alpha = 12$ . TABLE III shows the proposed method has a higher accuracy than the other methods.

To verify the capability of positioning tumor edge of the proposed method, we choose another five clinical tumor CT images (Fig.6 (a1-a5)). The parameters are identical with the CT-1 except that  $T_{a1} = T_{a2} = 0.46$  and  $T_{a3} = T_{a4} = T_{a5} = 0.36$ . The second column of Fig. 6 shows the proposed segmentation results and the third column is the manual tumor segmentation. It can be seen that the proposed method is close to the desired manual segmentation. TABLE IV shows the TM of the proposed method for different images, and the average TM value is 0.9187, which indicates the proposed method has higher segmentation accuracy.

TABLE.IV  
TM OF DIFFERENT METHODS

Image	Watershed with region merging	Marker-controlled watershed	Proposed method
CT-1	0.8403	0.8149	0.8883

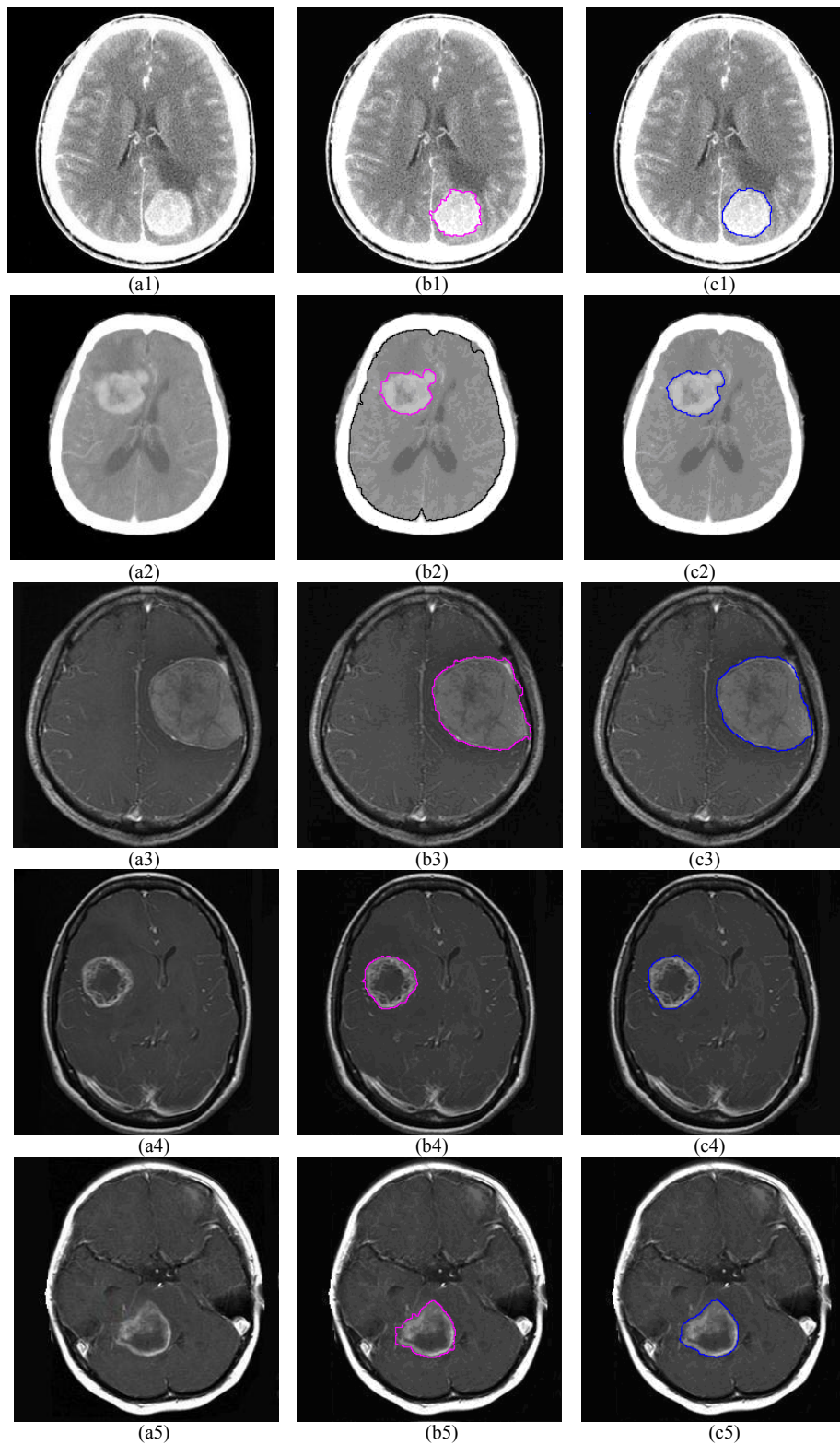


Figure6. Segmentation results of different images. (a) The original images; (b) The proposed method segmentation results; (c) Manual segmentation.

## VI. CONCLUSION

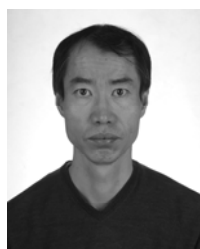
Brain tumor segmentation plays an important role in the treatment. We propose a hybrid method which combines morphological image modification and marker-controlled watershed transform to segment the brain tumors. The original image is modified by opening-closing with the constructed structuring element map to release the bright and the dark regular details while preserve the objects contour with less offset. Marker-controlled watershed transform is used to localize and segment the tumors. Synthetic and several clinical images experimental results show that the proposed method can release the over-segmentation of the traditional watershed, and allows reliable and precise segmentation of the brain tumors.

## ACKNOWLEDGEMENTS

This work was supported by the National Natural Science Foundation of China (61261029, 61202314), The Science and Technology Support Plan of Gansu Province (1204GKCA051), and Jinchuan Company Research Foundation (JCY2013009).

## REFERENCES

- [1] S.D. Salman and A.A. Bahrani, "Segmentation of tumor tissue in gray medical images using watershed transformation method," *Intl. Journal of Advancements in Computing Technology*, Vol. 2, No. 4, 2010, pp.123-127.
- [2] T. Wang, I. Cheng, A. Basu. "Fluid vector flow and applications in brain tumor segmentation," *IEEE Transactions on medical Engineering*, Vol. 53, No. 3, 2009, pp.781-789.
- [3] J.J Corso, E Sharon, A. Yuille, "Multilevel segmentation and integrated Bayesian model classification with an application to brain tumor segmentation," *Med. Image Comput. Comput. Assisted Intervention*, vol. 2, 2006, pp. 790-798.
- [4] J. H Liu, J. W Wang, "Research on Contour Correction in Medical CT", *Journal of Computers*, Vol. 7, No. 3, 2012, pp. 762-767.
- [5] KARANTZALOS K, ARGIALAS D. "Improving edge detection and watershed segmentation with anisotropic diffusion and morphological levellings". *International Journal of Remote Sensing*, Vol. 27, No.24, 2006, pp. 5427-5434.
- [6] J.H Li, "Morphological Segmentation of 2-D Barcode Gray Scale Image", *Journal of Computers*, Vol. 8, No. 10, 2013, 2461-2468.
- [7] V. Grau, A. U. J. Mewes, M. Alcañiz, R. Kikinis, and S. K. Warfield, "Improved watershed transform for medical image segmentation using prior information," *IEEE Transactions on Medical Imaging*. Vol. 23, No.4, 2004, pp. 447-458.
- [8] J. M. Sharif, M. F. Miswan, M. A. Ngadi, Md Sah Hjsalam. "Red blood cell segmentation using masking and watershed algorithm: A preliminary study," *Proceedings of 2012 International Conference on Biomedical Engineering (ICOBEB)*, 2012, pp. 258-262.
- [9] J. Cousty, G. Bertrand, L. Najman, Michel Couprie. "Watershed Cuts: Thinnings, Shortest Path Forests, and Topological Watersheds," *IEEE Transactions on Pattern Analysis and Machine Intelligence*, Vol. 32, No.5, pp. 925-939, 2010.
- [10] S. V Kumar, M. N Lazarus, C. Nagaraju, "A novel method for the detection of microcalcifications based on Multi-scale morphological gradient watershed segmentation algorithm," *International Journal of Engineering Science and Technology*, Vol. 2, No.7, 2010, pp. 2616-2622.
- [11] S. Xu, H. Liu, E Song, "Marker-controlled watershed for lesion segmentation in mammograms," *Journal of Digital Imaging*, Vol. 24, No.5, 2011, pp. 754-763.
- [12] B. Peng, L. Zhang, D. Zhang. "Automatic Image Segmentation by Dynamic Region Merging." *IEEE Transactions on Image Processing*, Vol. 20, No.12, 2011, pp. 3592-3605.
- [13] J. J. Corso, E. Sharon, S. Dube. "Efficient Multilevel Brain Tumor Segmentation with Integrated Bayesian Model Classification," *IEEE Transactions on Medical Imaging*, Vol. 27, No.5, 2008, pp. 629-640.
- [14] M. K. Kowar, S. Yadav, "Brain tumor detection and segmentation using histogram thresholding," *International Journal of Engineering and Advanced Technology*, Vol. 1, No.4, 2012, pp. 16-20.
- [15] M. C. Jobin Christ, R. M. S. Parvathi, "Segmentation of medical image using K-Means clustering and marker controlled watershed algorithm," *European Journal of Scientific Research*. Vol. 71, No.2, 2012, pp. 190-194.
- [16] N. Bouaynaya, D. Schonfeld, "Theoretical foundations of Spatially-Variant mathematical morphology part II: Gray-Level images," *IEEE Transactions on Pattern Analysis and Machine Intelligence*. Vol. 30, No.5, 2008, pp. 837-850.
- [17] C.Vachier, F. MEYER, "The viscous watershed transform," *Journal of Mathematical Imaging and Vision*, Vol. 22, No.2, 2005, pp. 251-267.
- [18] J. Ning, L.Zhang, D. Zhang and C. Wu, "Interactive Image Segmentation using Maximal Similarity based Region Merging," *Pattern Recognition*, Vol. 43, No.2, 2009, pp. 445-456.
- [19] L.L Xu and H.X Lu, "Automatic Morphological Measurement of the Quantum Dots Based on Marker-Controlled Watershed Algorithm", *IEEE Transactions on Nanotechnology*, Vol.12, No. 1, 2013, pp. 51-56.
- [20] S. H. Lewis, A J Dong, "Detection of Breast Tumor Candidates Using Marker-controlled Watershed Segmentation and Morphological Analysis", *SSIAI2012*, 2012, pp.1-4.
- [21] C.Y Lui, "Gaussian Kernelized Fuzzy c-means with Spatial Information Algorithm for Image Segmentation", *Journal of Computers*, Vol. 7, No. 6, 2012, pp. 1511-1518.



**Xiaopeng Wang** received his Ph.D degree in signal and information processing from Northwestern Polytechnical University, China, in 2005. His interested research fields are image analysis and recognition.



**Shengyang Wan** received his BA degree in electronic and Information engineering from Nanchang HangKong University, China, in 2010. He is currently pursuing an MS. degree in Signal and Information Processing at Lanzhou Jiaotong University, China. His research interests include image processing and pattern recognition.



**Lei Tao** received his Ph.D degree in information and communication engineering from the Northwestern Polytechnical University, Xian, in 2011. Currently, he is an Associate Professor at Lanzhou Jiaotong University. His research interests include image processing, pattern recognition and computer vision.